Relevance of single-particle and collective excitations in zirconium isotopes populated by neutron transfer reactions in the ^{90}Zr+^{208}Pb system

M. Varga Pajtler[a,*], S. Szilner[b], L. Corradi[c], G. de Angelis[c], E. Fioretto[c], A. Gadea[d], F. Haas[f], S. Lunardi[e], N. Mărginean[g], T. Mijatović[b], G. Montagnoli[e], D. Montanari[f], G. Pollarolo[h], F. Recchia[e], M. -D. Salsac[i], F. Scarlassara[e], N. Soić[b], A. M. Stefanini[c], C. A. Ur[e], J. J. Valiente-Dobón[c]

[a] *Department of Physics, University of Osijek, HR-31000 Osijek, Croatia*
[b] *Rudjer Bošković Institute, HR-10001, Zagreb, Croatia*
[c] *Istituto Nazionale di Fisica Nucleare, Laboratori Nazionali di Legnaro, I-35020 Legnaro, Italy*
[d] *IFIC, CSIC-Universidad de Valencia, E-46071 Valencia, Spain*
[e] *Dipartimento di Fisica, Universitá di Padova, and Istituto Nazionale di Fisica Nucleare, I-35131 Padova, Italy*
[f] *Laboratoire Pluridisciplinaire Hubert Curien, CNRS-IN2P3 and Université de Strasbourg, F-67037 Strasbourg, France*
[g] *Horia Hulubei National Institute of Physics and Nuclear Engineering, RO-077125 Bucharest-Magurele, Romania*
[h] *Dipartimento di Fisica Teorica, Universitá di Torino, and Istituto Nazionale di Fisica Nucleare, I-10125 Torino, Italy*
[i] *CEA, Centre de Saclay, IRFU/SPhN, F-91191 Gif-sur-Yvette, France*

Abstract

Neutron transfer channels have been studied in ^{90}Zr+^{208}Pb close to the Coulomb barrier energy in a fragment-γ coincident measurement employing the PRISMA - CLARA setup. The observed γ spectra of the zirconium isotopes ($^{89-94}$Zr) have been analysed and their level schemes have been revised. In general, a strong population of the yrast states, with energies ranging up to $\sim$ 7.5 MeV has been observed. New γ rays have been identified, and level schemes have been upgraded. The coupling of single-particle degrees of freedom to nuclear vibration quanta was discussed.

Keywords:
γ transitions and level energies, Transfer reactions, $59 \leq A \leq 89$, $90 \leq A \leq 149$
23.20.Lv, 25.70.Hi, 27.50.+e, 27.60.+j

*Corresponding author
Email address: mvarga@fizika.unios.hr (M. Varga Pajtler)

1. Introduction

The acceleration of heavy ions enables the collision of two complex systems, a dynamical process in which they are exchanging several quanta, of energy and angular momenta and of mass and charge [1, 2].

In this work we benefited from the use of multinucleon transfer reactions at energies close to the Coulomb barrier, the mechanism where many nucleons are transferred and where nuclear structure still plays a significant role in the dynamics (see Refs. [2, 3]). The revival of transfer reaction studies prospered from the construction of the new generation large solid-angle spectrometers based on trajectory reconstruction, that reached an unprecedented efficiency and selectivity. The coupling of these spectrometers with large γ arrays allowed the identification of individual transitions, their population pattern, and their decay modes via particle-γ coincidences.

A significant amount of experimental data on heavy ion transfer reactions collected in the last decade have been shown to be quantitatively described in the reaction model which includes elementary degrees of freedom, surface vibrations and single particles (see Refs. [2, 3] and references therein). It has been demonstrated that through the excitation of these elementary modes, the energy and angular momentum are transferred from the relative motion to these intrinsic degrees of freedom and that mass and charge are exchanged among the two partners of the collision. In this work, by the use of the heavy-ion transfer reactions in a particle-γ coincidence measurement, we will explore the couplings between the phonon degrees of freedom and those of the single particle.

In more details, the multineutron transfer reactions in ^{90}Zr+^{208}Pb, studied at energies close to the Coulomb barrier with the PRISMA-CLARA set-up, will be presented. The total yields for the pure neutron transfer channels collected in the PRISMA spectrometer have already been published [4]. These yields have been compared with the semi-classical model GRAZING [5, 6]. It turned out that the dependence of the cross sections on the number of transferred neutrons is very similar to the one observed in other studied systems (see for example [2, 7, 8, 9]). The neutron pick-up channels drop by almost a constant factor for each transferred neutron, as an independent particle mechanism would suggest. The large angular acceptance of PRISMA allowed the identification of neutron stripping channels, which are, for stable beams, strongly suppressed by optimum Q-value considerations. Here, one observes a drop in cross section of about one order of magnitude in moving from ^{90}Zr to ^{89}Zr.

In this paper, we will present the population pattern of the excited states of the zirconium isotopes populated via the neutron transfers. These patterns have been studied in the view of the coupling of single-particle degrees of freedom to nuclear vibration quanta, which is essential for the description of many basic states in the vicinity of closed shells. The effects of such coupling are largely unexplored, in particular, whether and to what extent a population of states of particle-phonon nature is present in isotopic chains reached via the same transfer mechanism. In fact, nuclear deformation and surface vibrations get increasing importance in moving from light to heavy ion transfer, where multi-

step processes may strongly modify the final strength distribution.

2. The experimental set-up and data analysis

The experiment ^{90}Zr+^{208}Pb has been performed with the XTU-Tandem + ALPI booster accelerator complex of the Laboratori Nazionali di Legnaro. The ^{90}Zr beam has been delivered at E_{lab}=560 MeV with an average intensity of 3 pnA onto a 280 μg/cm^2 ^{208}Pb (2 mm) strip target deposited on a 20 μg/cm^2 C-backing. Projectile-like products have been detected at two different angles, $\theta_{lab} = 56^\circ$ and $\theta_{lab} = 61^\circ$ with the PRISMA spectrometer.

The magnetic spectrometer PRISMA has a solid angle of $\simeq$ 80 msr ($\pm 6^\circ$ horizontal and for $\pm 11^\circ$ vertical) and a wide momentum acceptance of $\pm$10%. It consists of a magnetic quadrupole singlet and a magnetic dipole, and complex detector system: the micro-channel plate (MCP) [10] at the entrance, and the multi-wire parallel plate avalanche counter (MWPPAC) [11] at the focal plane, both position-sensitive with 1 mm resolutions. The MCP and MWPPAC provide the timing signal, with sub-nanosecond resolution, for the time-of-flight (TOF) determination. They are followed by the transverse field multiparametric ionization chambers (IC). The MWPPAC and the IC are segmented into several sections, to preserve a high resolution even when detection rates overcome several kHz. The IC has a very large size to stop all ions collected at the focal plane, whose kinetic energies may differ by more than 20%, given the large acceptance of the spectrometer. The segmentation of the anode into 40 rectangular sub-anodes allows to optimize the gas pressure in order to get the best nuclear charge resolution.

The described detector system gives all the necessary information for the complete ion identification, which is performed via an event-by-event reconstruction of the trajectory inside the magnetic elements [4, 12]. In this reconstruction, the ion trajectories after quadrupole are assumed to be planar, as a consequence of the fact that the longitudinal dimension of the PRISMA is much larger then the transversal one. In addition, due to the large dimensions of the magnetic elements, the fringing fields can been neglected. These assumptions have been carefully checked with the simulation of the ion transport through the spectrometer [12]. The trajectories are, thus, uniquely determined by the known ratio of the quadrupole and dipole magnetic fields, and the bending radius in the dipole (and consequently the total trajectory length) which is the result of the tracking procedure. These quantities: the know magnetic field, bending radius and total length, together with the measured TOF, provide the ratio A/q, being the A mass of the ion, and q its charge state. By plotting this quantity as a function of the horizontal position at the focal plane a characteristic repetitive pattern of the different A/q is obtained. One observes a rich and broad charge state distribution, characteristic of heavy ions. To disentangle the actual mass, the information of the total energy of the ions has been used. This total energy E is provided by the IC, which also measures the energy loss ΔE for the identification of the nuclear charge Z.

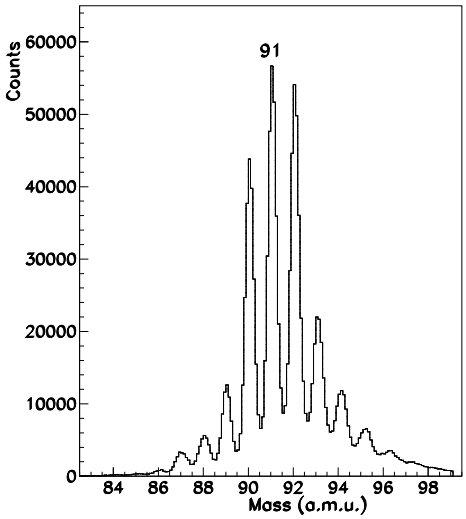

Figure 1: The mass distributions of Zr isotopes obtained with the condition that at least one γ ray was detected in the CLARA array.

Figure 1 shows the mass spectra of the zirconium isotopes, where a clear separation is visible with the mass resolution of $\Delta M/M \approx 1/230$. The represented spectrum is obtained with the condition that at least one γ ray was detected in the CLARA array. One sees the dominance of neutron pick-up channels, with a weaker population of neutron stripping channels, as expected from the optimum Q-value arguments. One also observes the suppression of the mass 90, i.e. ^{90}Zr, due to the elastic scattering.

CLARA γ-array [13] consisted of 24 clover detectors placed on a hemisphere (covering a solid angle of 2π) at the target position and opposite of PRISMA. Each clover detector was composed of four HP-Ge crystals surrounded by an anti-Compton shield, ensuring a peak-to-total ratio of $\approx 45\%$. The total photopeak efficiency was of the order of $\approx 3\%$ for 1.33 MeV γ-ray energy. The energy resolution obtained after the Doppler correction based on the knowledge of the reconstructed velocity vector in PRISMA was $\sim$ 0.6% - 0.9% over the whole velocity distribution of the projectile-like products detected in PRISMA.

Exploiting the binary character of the studied reaction, the velocity vector of the undetected heavy partner can be evaluated and applied for the Doppler correction of its corresponding γ rays. As an example, Fig. 2 shows the two-dimensional matrix of the γ spectra of ^{90}Zr and of ^{208}Pb, its heavy binary partner. As visible in the spectra, the γ rays belonging to the both partners are present. In fact, in the spectra of the light-partner, the wrongly Doppler corrected γ rays of the associated binary partner will appear as a very wide peak, and *vice versa*.

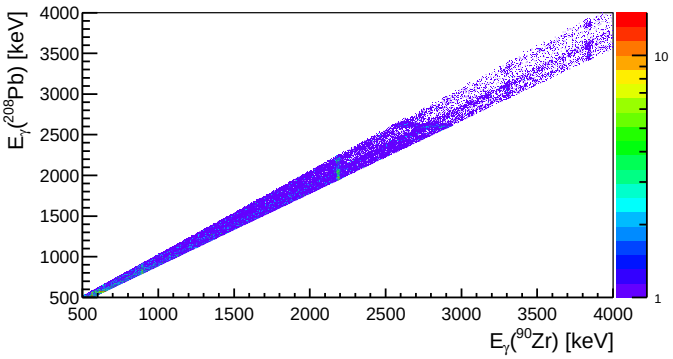

Figure 2: The two-dimensional matrix of the γ spectra Doppler corrected according to the reconstructed velocity of the ^{90}Zr detected in PRISMA (x axis) and of the ^{208}Pb, Doppler corrected according to the evaluated vector velocity, assuming the binary reaction) (y axis).

The strongest populated neutron transfer channels of the ^{90}Zr+^{208}Pb reaction are those of the ^{90,91,92}Zr isotopes, with the still sufficient statistics for the γ analysis of the ^{89,93,94}Zr isotopes. In the following section we will concentrate on the strongest populated states in the Zr isotopes, whose γ-ray spectra are plotted in Fig. 3.

In the case of the studied reaction mechanism, the bombarding energy has to be kept close to the Coulomb barrier as a compromise between having high primary cross sections and reasonable final yield. It is very difficult to preserve the good charge resolution for the direct detection of these low-energy heavy ions. This resulted in a contamination of some Zr spectra, i.e. some γ rays that do not necessarily belong to a given isotope appear in the spectra of that isotope. By comparing spectra of different zirconium isotopes with each other, and by comparing them with spectra of ytrium ($-1p$ channels) isotopes, we detected some overlap between nearby charges or masses. To clean spectra in a safe way, we scaled the spectrum that contains a γ ray which has been attributed to the close by isotope or isobar, and subtracted, in the whole energy range, the scaled spectrum from the one of interest. Here, we have to emphasize that the cleaning procedure does not significantly affect the number of counts for the γ transitions that belong to the detected isotope.

In the discussion of the strongest populated states and their dominant structure, we will take an advantage of the already published shell model calculations [14, 15]. Several newly observed γ rays will be presented and the level schemes will be updated based mainly on systematics with neighboring nuclei. This method was successfully used in different cases [16, 17, 18, 19], where electromagnetic transitions coming from the decay of specific nuclei have been identified by exploiting the fragment-γ coincidence measured in the PRISMA-CLARA set-up.

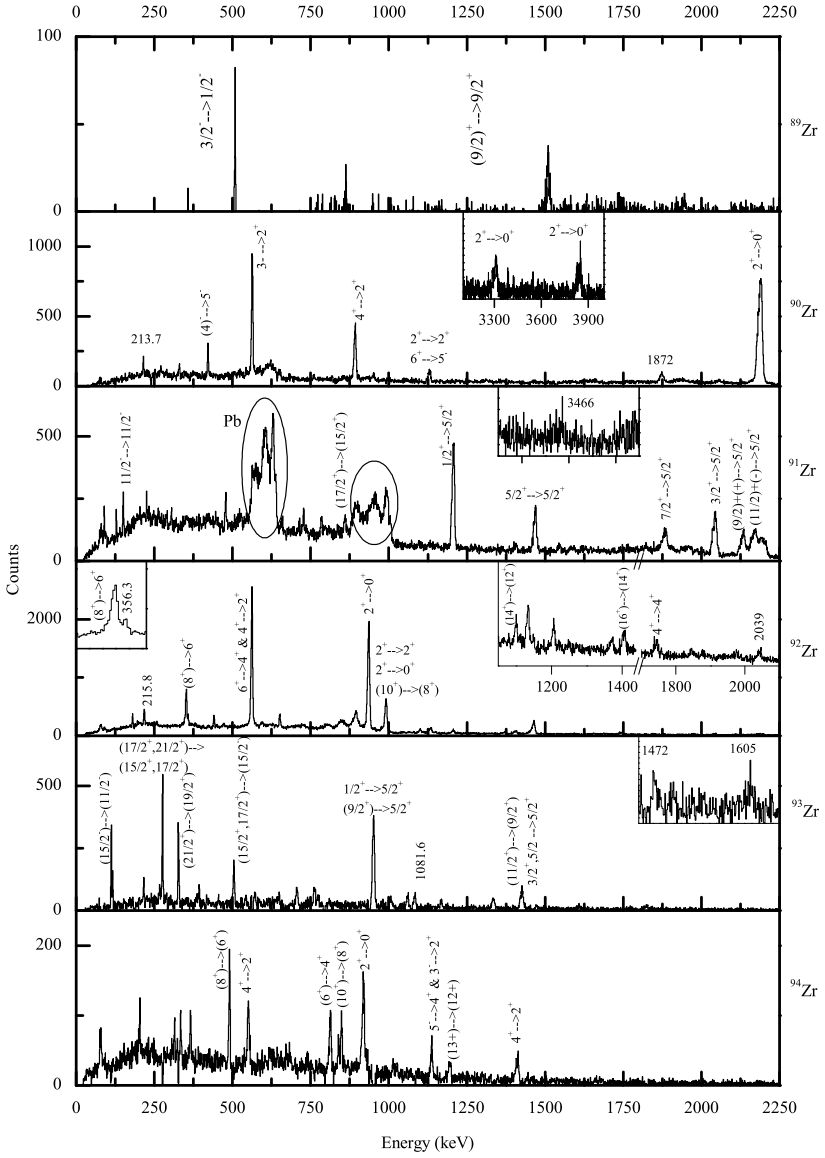

Figure 3: Doppler corrected γ-ray spectra of the observed Zr isotopes, $^{89-94}$Zr from top to bottom, respectively. Spins and parities (as in [20]) of initial and final states of the strongest transitions are tagged. The γ rays which could not be placed in the level scheme are labeled by their energies. The wrongly Doppler corrected γ rays of the heavy fragment are also labeled (see text).

3. Results and discussions

Based on the γ rays observed in our measurement, and the adopted energy, spin and parity of levels [20], level scheme of each isotopes has been constructed and updated. They are presented in Figs. 4, 5, and 6 (even-even isotopes) and 8, 9, and 10 (even-odd isotopes). The width of the arrow corresponds to the intensity of the observed γ ray corrected for the efficiency of the CLARA array. In some cases, when excited states have a complex decay pattern, with the transitions of different intensities, in weaker Zr channels we mostly observed only the strongest decay branch. We carefully checked that the expected number of events for these weaker (not observed) branches is consistent with the observed background level. For the decay of the states with the life-time longer than the time needed for ions to reach the focal plane of PRISMA, no coincidence between a fragment and prompt γ ray has been detected. These γ rays are depicted by dashed lines in Figs. 4, 8, and 9.

3.1. Even-even Zr isotopes

In general, in the even-even Zr isotopes (Figs. 4, 5 and 6), the strongest observed transitions are those from the decay of yrast states. In particular, in the ^{92}Zr, the $+2n$ channel, states up to spin $16\hbar$ and excitation energy of about 7.5 MeV were clearly identified. In the negative parity band, a strong excitation of 3^-, 5^- and 7^- states has been observed. Besides the yrast states, only higher order 2^+ and 4^+ states have been identified, although with lower intensities.

The observed population of the high excitation energy and spin states is closely connected with the character of the transfer mechanism, which, at this low bombarding energy tends to maximize the transferred angular momentum [2]. The similar situation has also been observed for the lighter systems [17, 4, 18].

Table 1: New γ transitions identified in the ^{90}Zr+^{208}Pb reaction. The first column lists energies of γ rays (E_γ) in keV obtained in here presented measurement, the second and third columns show energies (E_i), spins and parities (J_i^π) of suggested initial states, while energies (E_f), spins and parities (J_f^π) of suggested final states are listed in the fourth and fifth columns, as reported in [20].

isotope	E_γ (keV)	E_i (keV)	J_i^π	E_f (keV)	J_f^π
^{90}Zr	213.7(4)				
	1872(1)	4062(5)	4^+	2186.274(15)	2^-
^{91}Zr	3466(3)	3469(5)	$7/2^+$	0.0	$5/2^+$
^{92}Zr	215.8(4)				
	356.3(5)				
	2039(2) ?				
^{93}Zr	1081.6(7)	2025(10)	$9/2^-$, $11/2^-$	947.09(8)	$1/2^+$
	1472(1)	1463(5)	$7/2^+$, $9/2^+$	0.0	$5/2^+$
	1605(1)	1598(5)	$7/2^+$, $9/2^+$	0.0	$5/2^+$

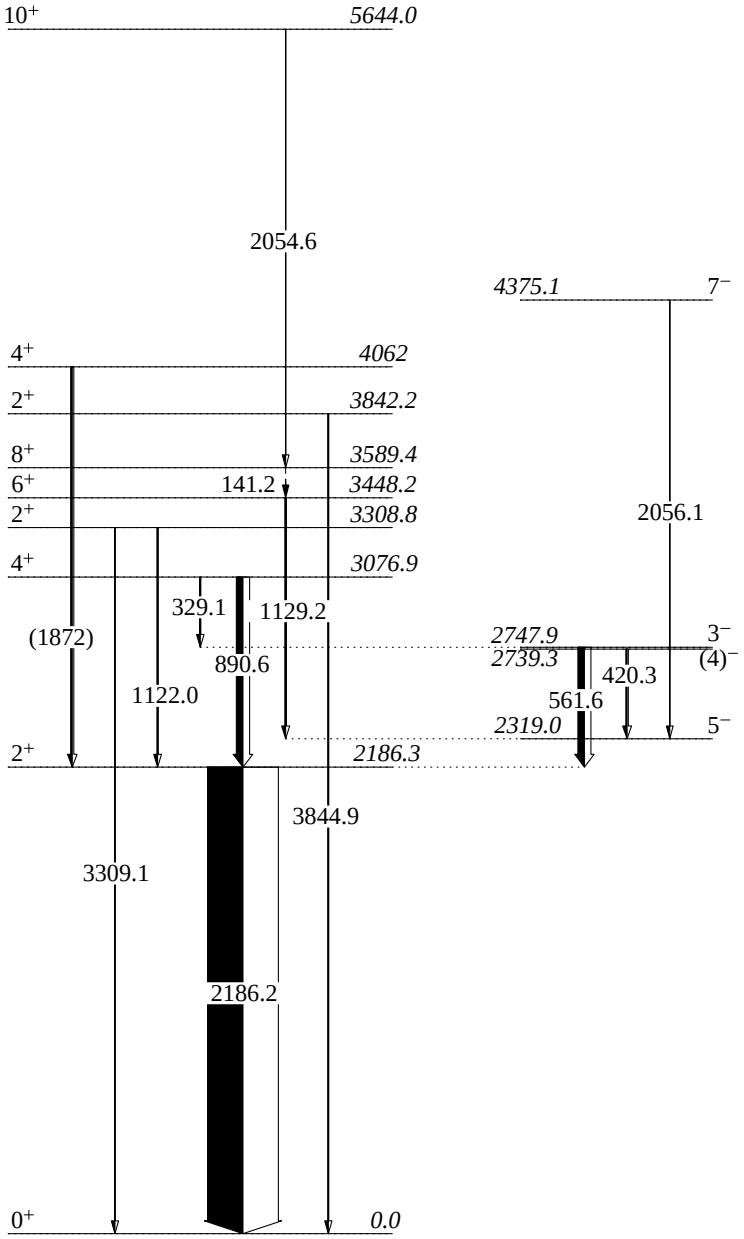

Figure 4: The experimental positive (left) and negative (right) parity states observed in our measurement for ^{90}Zr. Relative γ-ray intensities are indicated by the width of the arrow. The energy, spin and parity of levels, their branching ratios, and energy of transitions, are as in Ref. [20]. The γ ray denoted by dashed line hasn't been observed in the experiment (see text). The newly observed γ ray is denoted in parentheses (see text).

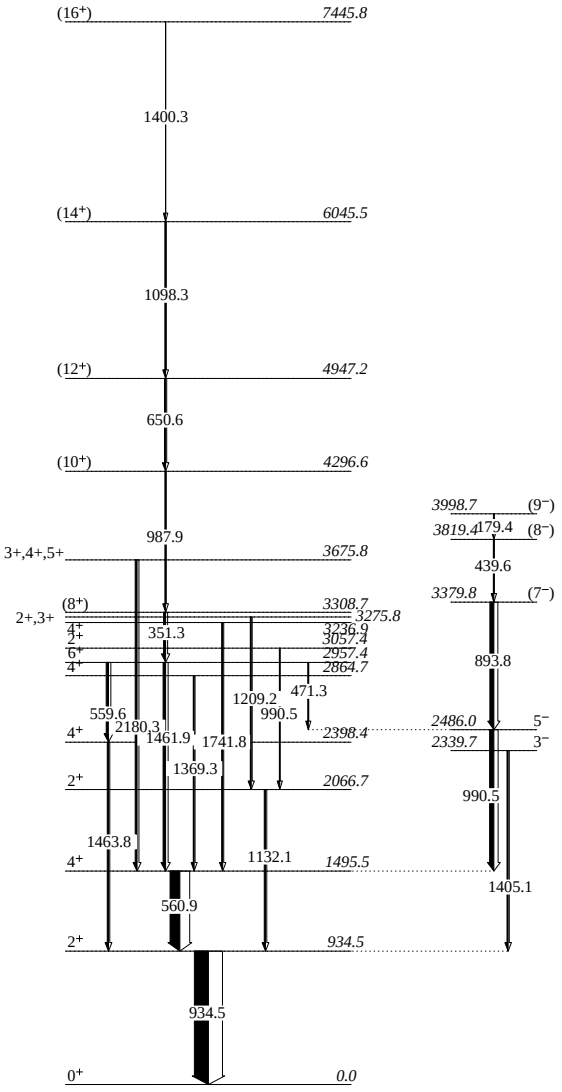

Figure 5: The experimental positive (left) and negative (right) parity states observed in our measurement for ^{92}Zr. Relative γ-ray intensities are indicated by the width of the arrow. The energy, spin and parity of levels, their branching ratios, and energy of transitions, are as in Ref. [20].

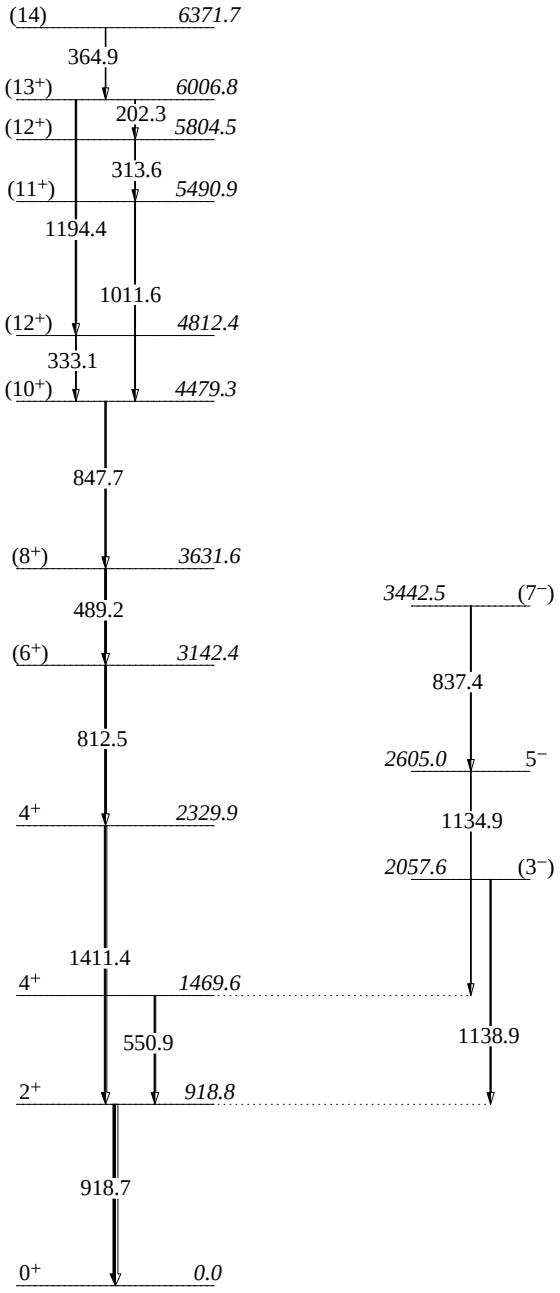

Figure 6: The experimental positive (left) and negative (right) parity states observed in our measurement for ^{94}Zr. Relative γ-ray intensities are indicated by the width of the arrow. The energy, spin and parity of levels, their branching ratios, and energy of transitions, are as in Ref. [20].

New γ transitions have been observed (see also Table 1), E_γ =213.7(4), and 1872(1) keV in ^{90}Zr, E_γ =215.8(4) keV, 356.3(5) keV, and 2039(2) keV in ^{92}Zr. For E_γ =1872 keV of ^{90}Zr we propose the transition from 4^+ at $E_{\rm ex} = 4062(5)$ keV to 2^+ at $E_{\rm ex} = 2186.274(15)$ keV. This assignment is in agreement with the fact that a similar pattern, i.e. excitation of the second order 2^+ and 4^+ states, has been observed in inelastic channel, in particular in (here not discussed) ^{208}Pb binary partner. This transition has been added to the level scheme of ^{90}Zr in Fig. 4.

For the assignment of these new γ transitions, we took advantage of the total kinetic energy loss (TKEL) for each of these transfer channels. The angle integrated total kinetic energy loss are constructed by assuming pure binary reaction. A selection of the populated states can be achieved by setting different gates on the TKEL distribution, as illustrated in Ref. [4]. Applying the same procedure here, it turned out that E_γ = 1872 keV is more pronounced for the low TKEL, while the unknown γ transitions E_γ = 213.7 keV in ^{90}Zr, and E_γ = 215.8, 356.3 keV in ^{92}Zr, are more pronounced for the large energy losses.

In ^{90}Zr, E_γ=213.9 keV has been observed in the fusion evaporation studies, via the ^{76}Ge(^{18}O, $4n\gamma$)^{90}Zr reaction, as a decay of a high-spin, high-excitation-energy state $(13)^+$ at 7437.8 keV [21]. The highest spin and excitation energy state observed in our measurement for ^{90}Zr, for which we were able to follow the cascade towards the ground state is the 10^+ state at 5644.03 keV. The states between the $(13)^+$ at 7437.84 keV and 10^+ at 5644.03 keV, decay either via a complex patterns where the total flux spreads over several γ transitions or via high energy γ transitions, for which the CLARA array is not very efficient. Thus it is very plausible, that the 213.7 keV transitions belongs to this high-spin, high-excitation-energy state, $(13)^+$ at 7437.8 keV, even if the complete cascade towards ground state has not been observed.

Thus it is our opinion that these low energy γ transitions may arrive from the decay of the higher excitation energy and high spin states in ^{90}Zr and ^{92}Zr. Of course, for the proper assignment, further studies are necessary.

To have a better insight in these new γ transitions identified in the ^{90}Zr+^{208}Pb reaction, we compared, when possible, the γ spectra with those obtained in the ^{40}Ca+^{96}Zr reaction [4, 22]. The ^{40}Ca+^{96}Zr was measured by accelerating a ^{40}Ca beam on a ^{96}Zr target, thus one has to keep in mind that the Zr spectra are the target-like spectra, where the velocity vector of these undetected heavy partners have been evaluated taking into account the binary character of the reaction. Hence, in the corresponding spectra, γ rays belong to both, the primary binary partner, as well as to the ones of the isotopes produced after evaporation takes place. For example, the ^{94}Zr spectrum, reached via the removal of two neutrons from the ^{96}Zr target in the ^{40}Ca+^{96}Zr reaction, is not necessarily the same as the ^{94}Zr spectrum reached via the pick-up of four neutrons on the ^{90}Zr beam in the ^{90}Zr+^{208}Pb reaction. The selected energy region of these two spectra are plotted in Fig. 3.1.

This energy region has been selected to better illustrate the different population of the high-spin states. It is clearly visible that in the case of the heavier system, i.e. ^{90}Zr+^{208}Pb, the transitions from higher spin states are more pro-

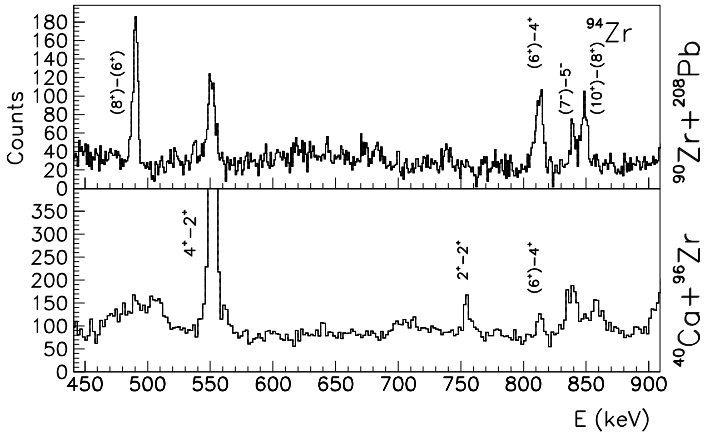

Figure 7: The ^{94}Zr γ spectra observed in the ^{90}Zr+^{208}Pb reaction (top) and in the ^{40}Ca+^{96}Zr reaction (bottom), for the energy region around 700 keV.

nounced (see for example the (8^+) to (6^+) and the (10^+) to (8^+) transitions). The similar situation was observed for the ^{92}Zr and ^{93}Zr isotopes.

The fact that in the case of the ^{92}Zr spectrum of ^{40}Ca+^{96}Zr the 2039 keV line is not so strongly populated speaks in favor of its high spin. The low-lying transitions (215.8, 356.3 keV) were not present in the ^{92}Zr spectrum from the ^{40}Ca+^{96}Zr reaction.

We would like to discuss at this point the possible population of the pairing-vibration states in even-even Zr isotopes. In the ^{90}Zr spectrum, in particular, one sees population of the nonyrast states up to energies $\sim$4 MeV. This excitation energy region is the region where the pairing vibration states are expected to occur [1]. In this region (with the very low background, see Fig. 3) one observes two peaks at E_γ=3844.9 keV and E_γ=3309.1 keV, corresponding to the decay to the ground state of non-yrast 2^+ states at the excitation energy 3842.2 and 3308.8 keV, respectively. Specific interest is coming from the study of the population strength of 0^+ in even-even isotopes in this excitation energy region. Therefore, we searched for possible decays of excited 0^+ states to 2^+ states populated in our measurement for the observed Zr isotopes, but we couldn't undoubtedly confirm the observation of any of these possible γ rays.

3.2. Even-odd Zr isotopes

Here, again as in the even-even isotopes, the transfer mechanism populates strongly the high spin states in both, positive and negative parity bands. It is interesting to notice that in the ^{91}Zr and ^{93}Zr (being the ^{89}Zr rather weak channel), above the excitation energy of $\sim$ 2.5 MeV, only the highest known

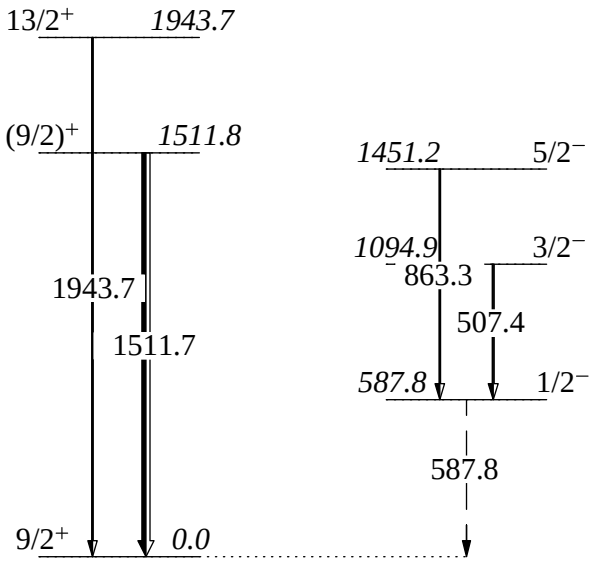

Figure 8: The γ transitions observed in our measurement for ^{89}Zr. Relative γ-ray intensities are indicated by the width of the arrow. The energy, spin and parity of levels, their branching ratios, and energy of transitions, are as in Ref. [20]. The γ ray denoted by dashed line hasn't been observed (see text). It decays from the long-lived ($T_{1/2}$=4.6 min) $1/2^-$ state.

spin states have been populated. This strongly speaks in favor of the selectivity of the transfer mechanism for the large angular momentum transfers.

In a simple shell model consideration (where the occupation probabilities for single-particle orbits are 0 or 1); the semi closed ^{90}Zr isotope has filled $g_{9/2}$ neutron orbital (the magic neutron number 50). Thus, in even-odd Zr isotopes one would expect that the ground states are well defined by the position of the unpaired neutron. In fact this is the case, in the ^{89}Zr, where a neutron hole defines its $9/2^+$ ground state, while an unpaired neutron in the $2d_{5/2}$ orbital defines the $5/2^+$ ground states in ^{91,93,95}Zr. Taking into account the neutron sub-shells in the $4\hbar\omega$, i.e. the $g_{7/2}$, $d_{5/2}$, $d_{3/2}$, $s_{1/2}$ or $h_{11/2}$ orbitals, one would expect the appearance of the $J^\pi = 7/2^+, 5/2^+, 3/2^+, 1/2^+$ and $11/2^-$ states, while the neutron hole in the $3\hbar\omega$ shell, with the $g_{9/2}$, $p_{1/2}$, $f_{5/2}$, $p_{3/2}$ or $f_{7/2}$ orbitals, would contribute to $J^\pi = 9/2^+, 1/2^-, 5/2^-, 3/2^-, 7/2^-$ states. These spins and parities dominate over the low-lying spectra of the even-odd Zr isotopes. Of course, the same spins can be also built with the different coupling, and their observation do not necessarily underline their possible single particle character.

Looking more closely at the ^{89}Zr (see Figs. 3 and 8), one would expect the dominance of the states due to the neutron hole in the $3h\omega$ shell, $J^\pi = 9/2^+$, $1/2^-$, $5/2^-$, $3/2^-$, and $7/2^-$. All of these states, except the highest excitation energy $7/2^-$ state, have been observed. In the recent large-shell model (SM) calculations [23] the structure of the Zr isotopes was discussed. In the employed

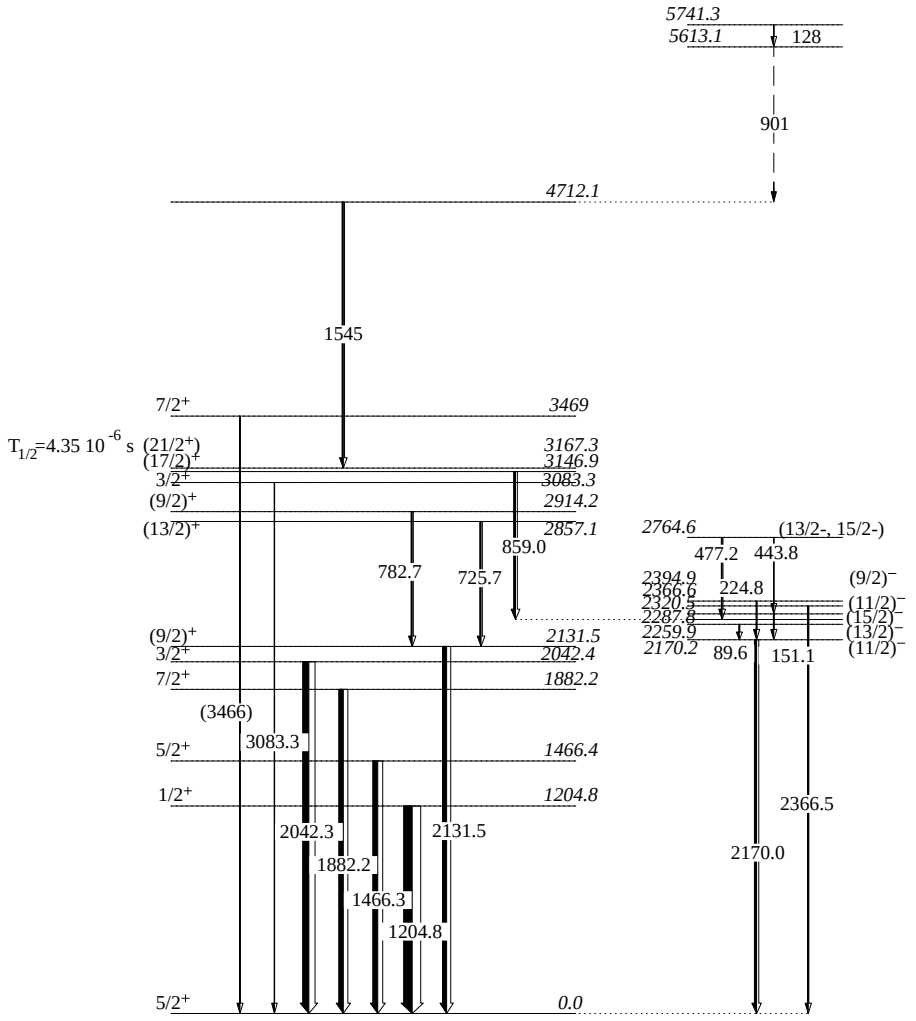

Figure 9: The experimental positive (left) and negative (right) parity states observed in our measurement for ^{91}Zr. Relative γ-ray intensities are indicated by the width of the arrow. The energy, spin and parity of levels, their branching ratios, and energy of transitions, are as in Ref. [20]. The intensity of the 901 keV γ transition could not be precisely extracted, as it overlaps with the wrongly Doppler corrected heavy-partner γ rays. Thus it is plotted as a dashed line. The newly observed γ ray is denoted in parentheses (see text).

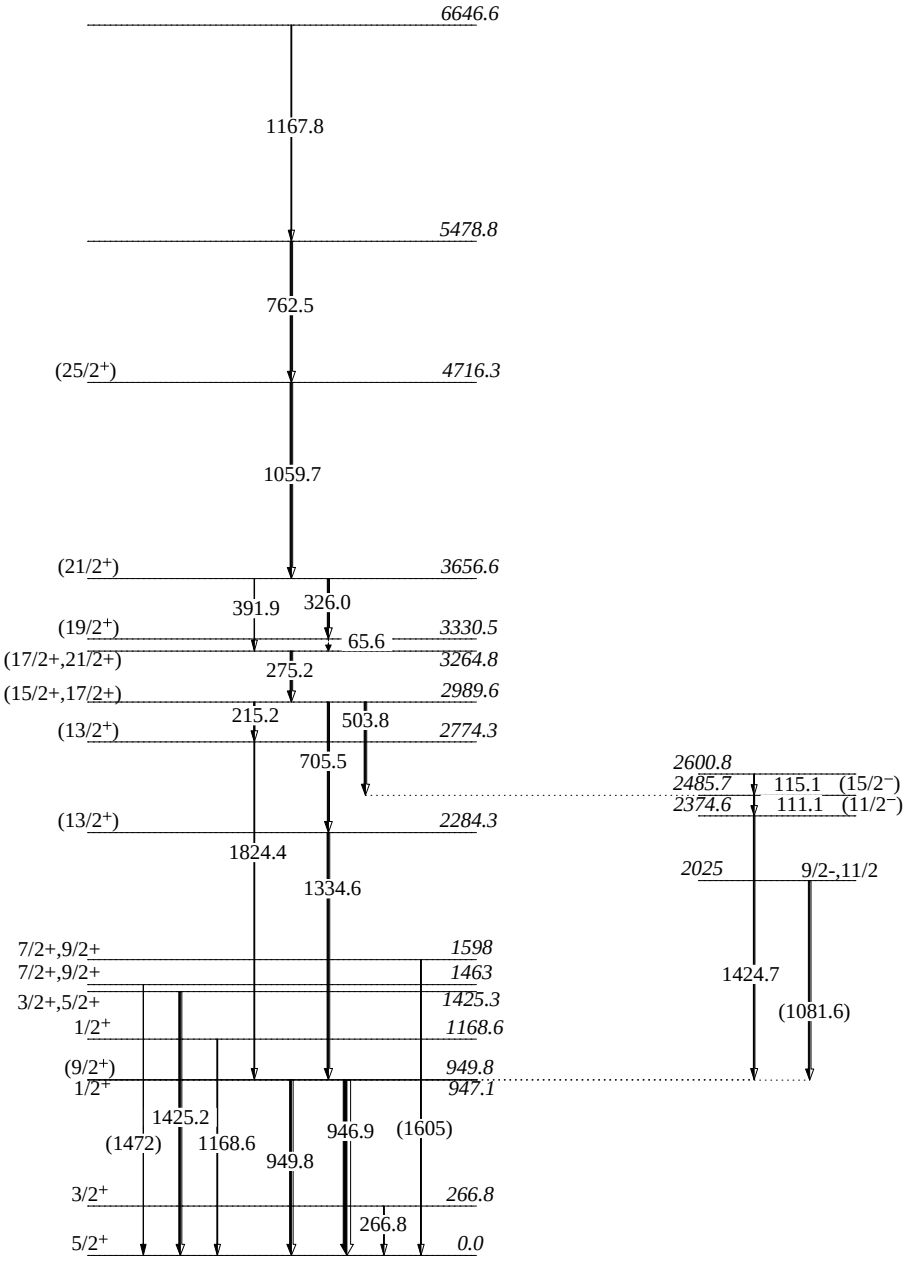

Figure 10: The experimental positive (left) and negative (right) parity states observed in our measurement for ^{93}Zr. Relative γ-ray intensities are indicated by the width of the arrow. The energy, spin and parity of levels, their branching ratios, and energy of transitions, are as in Ref. [20]. The newly observed γ rays are denoted in parentheses (see text).

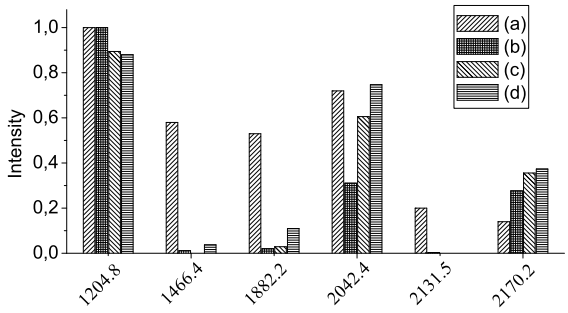

Figure 11: Population strengths of the levels of ^{91}Zr below the excitation energy 2180 keV (labeled with (a)), obtained in the $+1n$ channel of the ^{90}Zr+^{208}Pb reaction. These states are $1/2^+$ at 1204.8 keV, $5/2^+$ at 1466.4 keV, $7/2^+$ at 1882.2 keV, $3/2^+$ at 2042.4 keV, $(9/2)^+$ at 2131.5 keV and $(11/2^-)$ at 2170.2 keV. Data labeled (b), (c), and (d) have been extracted from the (d,p) reactions from Refs. [24, 25, 26], respectively.

SM calculations the doubly-closed nucleus $^{100}_{50}$Sn was assumed to be an inert core and the nuclei were described in terms of proton and neutron holes distributed in the $g_{9/2}$, $p_{1/2}$, $p_{3/2}$ and $f_{5/2}$ orbitals. These calculations demonstrated that the wave-functions of the $1/2^-$, $5/2^-$ and $3/2^-$ states (which are exactly the negative parity states observed in our measurement) have large components in which a neutron hole in the $p_{1/2}$ and $p_{3/2}$ orbitals is coupled to a proton configuration dominated by the $g_{9/2}$ orbital.

In the case of ^{91,93}Zr, one would expect that the states $9/2^+$, $7/2^+$, $3/2^+$, $1/2^+$ and $11/2^-$ will dominate over the spectra, beside the $5/2^+$ ground state. These states were, in fact, populated in the ^{91,93}Zr (see Figs. 9 and 10). To better explore the dominance of the single-particle character of the populated states in ^{91,93}Zr, we compared the population strengths obtained in here discussed measurement with strengths obtained in the (d,p) reactions, [24, 25, 26] for ^{91}Zr, and [27] for ^{93}Zr. In these light-ion induced transfer reactions, a strong population of the states of single-particle character is expected. This comparison for the ^{91}Zr is shown in Fig. 11.

The population strength of the ^{91}Zr levels, with the excitation energy below 2.8 MeV (see Fig. 11), has been obtained by subtraction of the feeding from above in agreement with the level scheme of Fig. 9, and corrected for the efficiency of the CLARA array. The intensity of each transition was normalized to the strongest transition (from $1/2^+$ to $5/2^+$). The ^{90}Zr$(d,p)^{91}$Zr reactions data have been extracted from the cross sections of the observed states [24], or by evaluating the spectroscopic factors [25, 26], and also normalized for the strongest transitions.

A similar comparison has been carried between the selected states of ^{93}Zr populated via the $+2n$ channel in the ^{90}Zr+^{208}Pb reaction, and in the ^{92}Zr$(d,p)^{93}$Zr reaction [27]. The analysis was also carried out for the energy level $E_{\rm ex} = 2025$ keV $(9/2^-,11/2^-)$ whose decay was unknown, and to which we attributed a

newly observed $E_\gamma = 1081.6$ keV.

In these comparisons we observed that the $1/2^+$ and $3/2^+$ states in ^{91}Zr have similar strengths in the both, light and heavy ion induced reactions, while the higher spin states, $5/2^+$, $7/2^+$ and $9/2^+$ are strongly excited in the ^{90}Zr+^{208}Pb reaction. In contrast to light-ion induced reactions, the large part of the flux of the ^{90}Zr+^{208}Pb reaction is in the negative parity states. Concerning the negative parity states, in the (d,p) reaction, only the $(11/2)^-$ at 2170.2 keV has been populated. In the case of ^{93}Zr, similarly, the low spins have equal strength, while the population of the state $9/2^-$,$11/2^-$ at 2025(10) keV was strongly populated in heavy-ion induced reaction.

The shell-model calculations [15] carried out within the model space ($1f_{5/2}$, $1p_{1/2}$, $2p_{3/2}$, $1g_{9/2}$) for protons and ($2d_{5/2}$, $3s_{1/2}$, $2d_{3/2}$, $1g_{7/2}$, $1h_{11/2}$) for neutrons discussed the single-particle components of the low-lying states in ^{91}Zr. They demonstrated that the unpaired neutron occupies predominately a single orbital (occupation probability > 0.88) confirming the strong single-particle character of the low-lying $1/2^+$, $5/2^+$ and $7/2^+$. It is interesting to notice that the occupation probability for the first $1/2^+$ state in the $\nu s_{1/2}$ is 0.976, and for the first $5/2^+$ states (the ground state and the first $5/2^+$ excited state) in the $\nu d_{5/2}$ is > 0.98, while the first $7/2^+$ state is mostly composed of the $d_{5/2}$ (occupation probability 0.885) with only a small contribution of the $\nu g_{7/2}$ orbital (0.1). The true $\nu g_{7/2}$ single particle state is expected at the higher energies.

New γ transitions have been, also, observed in the even-odd isotopes, 3466(3) keV in ^{91}Zr, 1081.6(7) keV, 1472(1) keV and 1605(1) keV in ^{93}Zr (see Table 1). The 3466 keV γ ray in ^{91}Zr, based on the energy difference between known energy levels, could be attributed to the transition from 3469(5) keV level ($7/2^+$) to the ground state. This state, whose γ decay was not know, has been populated with the similar strength as the $7/2^+_1$ state, in the light-ion induced one neutron transfer reactions ($(\alpha,^3\mathrm{He})$, (d,p), $(^{12}\mathrm{C},^{11}\mathrm{C})$ [25, 28, 26, 29]. The state was also excited in the different scattering measurement, (α,α'), (p,p'), (d,d'). This state probably corresponds to the $\nu g_{7/2}$ state, and its strong excitation is expected in the one neutron transfer reaction.

Looking at the neighboring odd Zr isotopes (^{91}Zr and ^{95}Zr) of ^{93}Zr, where the $7/2^+$ state decays to the ground state, we suggest that $E_\gamma = 1605$ keV in ^{93}Zr decays from the $7/2^+, 9/2^+$ (at 1598(5) keV) level in ^{93}Zr, where our preference is for the $7/2^+$ spin.

This state, $7/2^+, 9/2^+$ at 1598 keV was populated in the one neutron pick-up (^{92}Zr$(\alpha,^3\mathrm{He})$, ^{92}Zr(d,p)) and stripping (^{94}Zr(d,t)) reactions. The neutron pick-up reaction also (even with the large spectroscopic factor) populated the same spin-parity state at 1463(5) keV. The energy of our 1472 keV γ ray is close to the possible transition to the ground state, although outside of the quoted error. One should notice that this line, 1463 keV is more intense than the 1604.5 keV line, in agreement with the stronger excitation of the first $7/2^+, 9/2^+$ state. Taking into account the energy difference of adopted levels, the same transition, 1472 keV, may also be attributed to the decays of the higher lying $7/2^+, 9/2^+$ states observed in the light-ion induced reaction (1735(?), or 2638(10) keV) but as a large multipolarity decays. Thus, our preference is the attribution to the

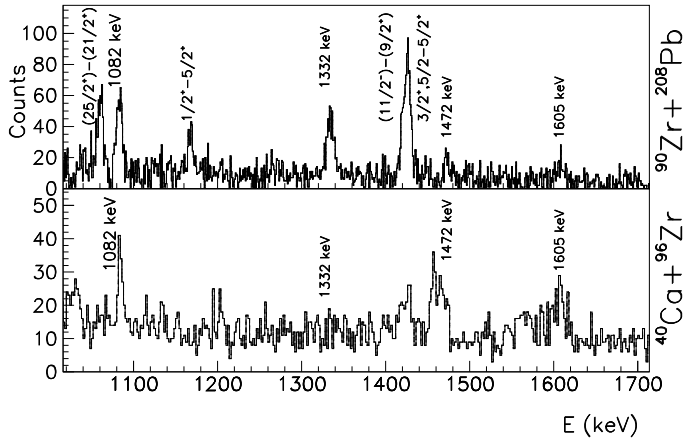

Figure 12: The ^{93}Zr γ spectra observed in the ^{90}Zr+^{208}Pb reaction (top) and in the ^{40}Ca+^{96}Zr reaction (bottom), for the energy region around 1200 keV.

lowest known $7/2^+, 9/2^+$ state.

In addition, we attributed the 1081.6 keV transition to the decay from the lowest negative parity state $9/2^-, 11/2^-$ at 2025 keV. This attribution is based on similarity with the level scheme of ^{91}Zr, where we observed high density of negative parity states with rather high spins. Since we noticed a resemblance between the level schemes of ^{91}Zr and ^{93}Zr (i.e. excitation of "single-particle" states in the lower energy part and selective population of higher spin levels), we expect to see the decay of $11/2^-$ to the ground state in ^{93}Zr, as it was the case in ^{91}Zr.

For these new transitions in the ^{93}Zr spectra, we carried out the TKEL analysis explained above, which revealed that they were more emphasized for the low-energy gate on TKEL. The level scheme has been thus updated with these new transitions.

We also compared the ^{93}Zr spectrum obtained in the ^{90}Zr+^{208}Pb reaction, with the one obtained in the ^{40}Ca+^{96}Zr reaction [4, 22]. This comparison, for the energy range of interest, is shown in Fig. 12. The 1605 keV transition appears stronger in the ^{40}Ca+^{96}Zr reaction, while the 1081.6 keV and 1472 keV lines are of similar strength in the both reactions.

Here we would like to remind about our previous finding concerning the $11/2^-$ state in ^{95}Zr in the ^{40}Ca+^{96}Zr reaction, where we reported the E3 transition of the $11/2^-$ state at 2025(7) keV [4]. The strong population of the $11/2^-$ state in all studied Zr isotopes will be discussed in more detail in the following paragraphs.

In the view of the dominant character of the states populated in our measurement, it is very convenient to look more closely at the dominant structure of

the populated $11/2^-$ states. From the point of view of studies of the structure of very neutron rich Zr isotopes, it is very important to establish the location of the $\nu 11/2^-$ orbital. Being the more neutron rich Zr isotopes difficult to reach, the knowledge about the position and decay pattern of the $11/2^-$ states is not always experimentally established.

These finding will be of large importance in the theoretical calculations, as they would ensure a correct evolution of the single-particle fields, going towards more neutron rich nuclei. The character of the states which originate from coupling of the 51st neutron to 2^+ and 3^- states in ^{91}Zr was discussed in the SM calculations [26]. Is was concluded that states with the same spin and parity, but based on different core states, mix strongly with each other and with single-particle states, and that the simple weak coupling model cannot be applied in the case of ^{91}Zr, and especially for the coupling to the 3^- phonon. A major fraction of the $h_{11/2}$ single-particle component in these calculations was contained in the $(11/2)^-$ state at 2.170 MeV, the state which was strongly excited in the (p, p') reaction.

In the more recent SM calculations [14], the evolution of the $11/2^-$ states in Zr isotopes was extensively discussed. These SM calculations were performed in an extended shell model space ($1f_{5/2}$, $2p_{1/2}$, $2p_{3/2}$, $1g_{9/2}$) for protons and ($2d_{5/2}$, $3s_{1/2}$, $2d_{3/2}$, $1g_{7/2}$, $1h_{11/2}$) for neutrons. The dimension of such configuration space overcome in general the present computational possibilities, thus it is of great importance to study the possible truncation schemes. In addition, the effective interaction for this valence space has to be established. The both procedures have to ensure the proper evolution of the single-particle fields, and at the present, the largest uncertainties are in the high-spin states that involve excitations to the $h_{11/2}$ orbital. A fair agreement with experiment is found in ^{91,93,95}Zr for all calculated states. In ^{91}Zr, it has been demonstrated that the $11/2^-$ (at $\sim$2.1 MeV experimentally and theoretically) state has a dominant $\pi(p^1_{1/2}g^1_{9/2})$ $\nu(d^1_{5/2})$ component (55%). Even more, the total number of neutrons in the $h_{11/2}$ was calculated to be only 0.16. Similarly, for $11/2^-$ at $\sim$2 MeV in ^{93}Zr, the dominant configuration turned out to be very similar: $\pi(p^1_{1/2}g^1_{9/2})$ $\nu(d^3_{5/2})$ with the $h_{11/2}$ orbital occupancy of 0.27%. Only in ^{97}Zr, the calculated low-lying $11/2^-$ level acquires a single-particle nature, due to the $d_{5/2}$ closure.

4. Fermion-phonon coupling

As already stated previously, the coupling of single-particle degrees of freedom to nuclear vibration quanta is essential for the description of many basic states in the vicinity of closed shells. The experimental yields of the ^{90}Zr+^{208}Pb reaction have been compared with the model that explicitly treats the internal degrees of freedom of the two ions in terms of surface vibration and single particles [4]. The excitation and transfer processes are mediated by the well-known single-particle form factors for the fermion degrees of freedom and by the collective form factors for the vibrational modes.

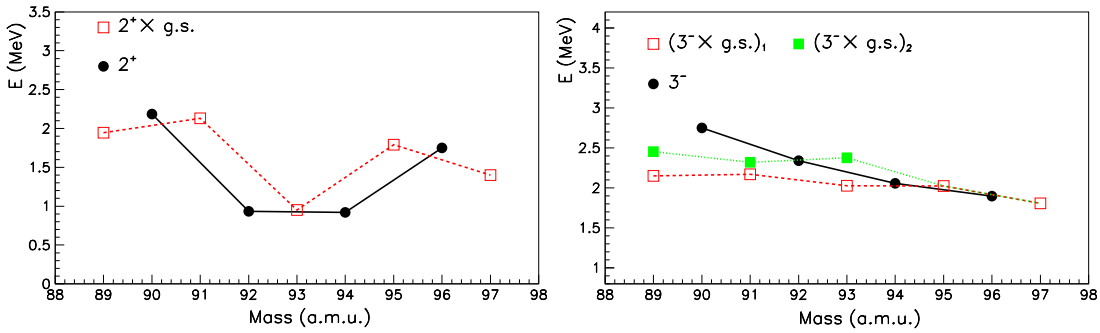

Figure 13: Right panel: energies of the first 2^+ states (solid circles) in even-even Zr isotopes, together with energies of the $13/2^+$ state in ^{89}Zr, $9/2^+_1$ states in ^{91,93,95}Zr and $5/2^+$ in ^{97}Zr (open squares). Right panel: energies of the first 3^- states in even Zr isotopes (solid circles), and energies of the first $15/2^-_1$ in ^{89}Zr, $11/2^-_1$ in ^{91,93,95}Zr and $7/2^-_1$ in ^{97}Zr (open squares), and the second $15/2^-_2$ in ^{89}Zr, $11/2^-_2$ in ^{91,93}Zr (solid squares). Lines are here only to guide the eyes.

In this view we looked more closely to the possible fermion-phonon coupling nature of the states populated by the neutron transfer mechanism. In the case of the ^{91}Zr and ^{93}Zr nuclei, for the coupling of the $5/2^+$ ground states to the first 2^+, one expects a multiplet $9/2^+$, $7/2^+$, ... $1/2^+$, while by the coupling to a 3^-, one expects a $11/2^-$, $9/2^-$, ... $1/2^-$ multiplet. The reaction mechanism does not populate the components of the two multiplets uniformly but favors the stretched configurations, $9/2^+$ and $11/2^-$. The same argument holds for ^{89}Zr, where coupling of its $9/2^+$ ground state to 2^+ and 3^- would result in $13/2^+$ and $15/2^-$ stretched configurations, respectively. The properties of these particle-phonon states should be to a large extent determined by the properties of the corresponding phonon states. Thus, in Fig. 13 we plotted the energies of the first 2^+ and 3^- states in even-even Zr isotopes, together with the energies of the states with the expected stretched configuration of the ground-state-phonon coupling.

In the even-even Zr isotopes, the low-energy part of the spectrum is dominated by a 2^+ state and a higher lying 3^-. In ^{90,92,94,96}Zr, all the 2^+_1 states decay predominantly to the ground state, with the $B(E2)$ ranging from 0.055 b^2e^2 in ^{96}Zr to 0.008 b^2e^2 in ^{92}Zr. The decay pattern of the 3^- states changes considerably when going from ^{90}Zr to ^{96}Zr. The strongest decay branch is via the $E1$ transition to the 2^+ state. In ^{90}Zr, only about 4% goes via E3 decay to the ground state, while in ^{96}Zr that percentage rises to 19%. In the ^{94}Zr, 2.8% of the intensity belongs to the decay to 4^+_1 state. In the ^{92}Zr, the situation is more complicated; the E1 transition is still the strongest one, followed by a transition to the 4^+_1 ($\sim 30\%$) and 2^+_2 ($\sim 11\%$) states, being the E3 transition of a negligible strength ($\sim 0.1\%$).

This situation is repeated in odd-even isotopes. It was especially obvious in

the case of ^{95}Zr [4, 27, 30], where the distribution of strengths over E1 (100%) and E3 (20%) transitions of the $11/2^-$ state at 2021.6 keV was very similar to the one observed in ^{96}Zr. In ^{89}Zr, the known decay of the first $15/2^-$ state at 2150.6 keV is through $E_\gamma = 29.3$ keV ($I_\gamma = 100\%$) and $E_\gamma = 206.9$ keV ($I_\gamma = 42\%$). The 29.3 keV γ ray has a very low energy for the proper detection with CLARA, while the intensity of the second was to low for the weakly populated channel in our reaction. Regarding the ^{93}Zr nucleus, the decay pattern of the tabulated $11/2^-$ states is not well established. From the known decays, we observed the E1 transition of the $(11/2^-)$ state at 2374.6 keV, and possibly its E3 decay ($E_\gamma = 2375$ keV). However, the ratio of the number of events in the E3/E1 transitions is not as expected. From the other possible $11/2^-$ states, we searched for the possible E1 and E3 transitions of the states labeled as $9/2^-$,$11/2^-$ at 2025(10) keV and 2363(10) keV. In this case, we expect γ rays of E1 transitions with energies 1075 and 1413 keV, respectively. The expected E3 transitions would provide γ rays of 2025 and 2363 keV, respectively. In the uncorrected spectrum of ^{93}Zr (which we looked to increase statistics), we observed a peak at around 2367 keV, over a complex background. The expected E1 transition (1413 keV), overlaps with two relatively strong transitions in ^{93}Zr, $E_\gamma = 1334.6$ keV (with the intensity of $\sim 30\%$) and $E_\gamma = 1425.2$ keV ($\sim 40\%$). Thus, we cannot without a significant doubt demonstrate the decay of 2363 keV state (assumed to be $11/2^-$), via expected E1 and E3 transitions. (In the case of the state $9/2^-$,$11/2^-$ at 2025 keV, we did not observe expected E3 transition.)

A similar situation appears in the ^{91}Zr nucleus, where two $11/2^-$ states with similar energy can be found. By looking at the energy of these states in Fig. 13, it turned out that their behaviour is outside of the systematics. The 3^- collective states may correspond to a complex superposition of cross shell excitations (see also Ref. [14]), and the deviation of the systematics presented in Fig. 13 is due to the strong mixing of different configurations.

The structure of states excited in multinucleon transfer reactions has been studied in various experiments performed at PRISMA spectrometer so far (see for example Refs. [4], [16], [17], or [18]). It has been found in those experiments that, in addition to the strong excitation of states of single-particle character, the states whose underlying structure could be explained by fermion-phonon nature were strongly excited. Our results confirm these findings.

5. Conclusion

Multinucleon transfer reactions have been studied in the ^{90}Zr+^{208}Pb system close to the Coulomb barrier energy with the PRISMA - CLARA set-up, at the *Laboratori Nazionali di Legnaro-INFN* accelerator center. This fragment-γ coincident measurement uniquely attributes electromagnetic transitions to each nuclei identified in the PRISMA spectrometer. Presented results, in general, contribute significantly to the understanding of the selectivity of the multi-nucleon transfer reaction mechanism in the selection of the states of specific structure.

In all the observed nuclei (with the exception of ^{89}Zr, which is a weaker reaction channel), it is clear that most of the excited states belong to the yrast states, i.e. the states which have the highest spin for the given energy. In some isotopes, high spin states were selectively observed, showing that the multinucleon transfer reactions with heavy ions are a good tool to excite high spin and energy states.

In the study of the underlying structure of the strongly excited states we investigated the possibility of the coupling of the ground state of the odd Zr nuclei to the 2^+ or 3^- vibration quanta in the stretched configuration. The results show that in most of the studied isotopes, the decay modes and the energies of the 2^+ and 3^- states in even isotopes have similar decay modes and energies as the expected particle-vibration states in the odd nuclei.

A thorough examination of the γ spectra revealed that new γ transitions have been identified (which were not previously reported in [20]), and uniquely attributed to the specific isotope. When possible, decay patterns for these rays have been suggested and the level schemes have been updated based mainly on systematics with neighboring nuclei.

6. Acknowledgement:

The authors are grateful to the LNL Tandem-ALPI staff for the good quality beams and the target laboratory for the excellent target. This work was partly supported by the EC FP6Contract ENSAR No. 262010. This work has been supported in part by Croatian Science Foundation under the project 7194.

References

[1] R. Broglia, A. Winther, Heavy ion reactions, Addison-Wesley, Redwood City, CA, 1991.

[2] L. Corradi, G. Pollarolo, S. Szilner, Multinucleon transfer processes in heavy-ion reactions, Journal of Physics G: Nuclear and Particle Physics 36 (11) (2009) 113101.

[3] R. Broda, Spectroscopic studies with the use of deep-inelastic heavy-ion reactions, Journal of Physics G: Nuclear and Particle Physics 32 (6) (2006) R151.

[4] S. Szilner, C. A. Ur, L. Corradi, N. Mărginean, G. Pollarolo, A. M. Stefanini, S. Beghini, B. R. Behera, E. Fioretto, A. Gadea, B. Guiot, A. Latina, P. Mason, G. Montagnoli, F. Scarlassara, M. Trotta, G. d. Angelis, F. D. Vedova, E. Farnea, F. Haas, S. Lenzi, S. Lunardi, R. Mărginean, R. Menegazzo, D. R. Napoli, M. Nespolo, I. V. Pokrovsky, F. Recchia, M. Romoli, M.-D. Salsac, N. Soić, J. J. Valiente-Dobón, Multinucleon transfer reactions in closed-shell nuclei, Phys. Rev. C 76 (2007) 024604. doi:10.1103/PhysRevC.76.024604.

[5] A. Winther (2014). [link].
URL http://www.to.infn.it/$\sim$nanni/grazing

[6] A. Winther, Grazing reactions in collisions between heavy nuclei, Nuclear Physics A 572 (1) (1994) 191 – 235. doi:http://dx.doi.org/10.1016/0375-9474(94)90430-8.

[7] S. Szilner, L. Corradi, G. Pollarolo, S. Beghini, B. R. Behera, E. Fioretto, A. Gadea, F. Haas, A. Latina, G. Montagnoli, F. Scarlassara, A. M. Stefanini, M. Trotta, A. M. Vinodkumar, Y. Wu, Multinucleon transfer processes in ^{40}Ca $+^{208}$ Pb, Phys. Rev. C 71 (2005) 044610. doi:10.1103/PhysRevC.71.044610.

[8] L. Corradi, A. M. Vinodkumar, A. M. Stefanini, E. Fioretto, G. Prete, S. Beghini, G. Montagnoli, F. Scarlassara, G. Pollarolo, F. Cerutti, A. Winther, Light and heavy transfer products in ^{58}Ni+^{208}Pb at the coulomb barrier, Phys. Rev. C 66 (2002) 024606. doi:10.1103/PhysRevC.66.024606.

[9] L. Corradi, A. M. Stefanini, C. J. Lin, S. Beghini, G. Montagnoli, F. Scarlassara, G. Pollarolo, A. Winther, Multinucleon transfer processes in ^{64}Ni+^{238}U, Phys. Rev. C 59 (1999) 261–268. doi:10.1103/PhysRevC.59.261.

[10] G. Montagnoli, A. Stefanini, M. Trotta, S. Beghini, M. Bettini, F. Scarlassara, V. Schiavon, L. Corradi, B. Behera, E. Fioretto, A. Gadea, A. Latina, S. Szilner, L. Don, M. Rigato, N. Kondratiev, A. Y. Chizhov, G. Kniajeva, E. Kozulin, I. Pokrovskiy, V. Voskressensky, D. Ackermann, The large-area micro-channel plate entrance detector of the heavy-ion magnetic spectrometer {PRISMA}, Nuclear Instruments and Methods in Physics Research Section A: Accelerators, Spectrometers, Detectors and Associated Equipment 547 (23) (2005) 455 – 463. doi:http://dx.doi.org/10.1016/j.nima.2005.03.158.

[11] S. Beghini, L. Corradi, E. Fioretto, A. Gadea, A. Latina, G. Montagnoli, F. Scarlassara, A. Stefanini, S. Szilner, M. Trotta, A. Vinodkumar, The focal plane detector of the magnetic spectrometer {PRISMA}, Nuclear Instruments and Methods in Physics Research Section A: Accelerators, Spectrometers, Detectors and Associated Equipment 551 (23) (2005) 364 – 374. doi:http://dx.doi.org/10.1016/j.nima.2005.06.058.

[12] D. Montanari, E. Farnea, S. Leoni, G. Pollarolo, L. Corradi, G. Benzoni, A. Gadea, E. Fioretto, A. Latina, G. Montagnoli, F. Scarlassara, A. Stefanini, S. Szilner, Response function of the magnetic spectrometer prisma, The European Physical Journal A 47 (1). doi:10.1140/epja/i2011-11004-9.

[13] A. Gadea, D. Napoli, G. de Angelis, R. Menegazzo, A. Stefanini, L. Corradi, M. Axiotis, L. Berti, E. Fioretto, T. Kroell, A. Latina, N. Marginean,

G. Maron, T. Martinez, D. Rosso, C. Rusu, N. Toniolo, S. Szilner, M. Trotta, D. Bazzacco, S. Beghini, M. Bellato, F. Brandolini, E. Farnea, R. Isocrate, S. Lenzi, S. Lunardi, G. Montagnoli, P. Pavan, C. Rossi Alvarez, F. Scarlassara, C. Ur, N. Blasi, A. Bracco, F. Camera, S. Leoni, B. Million, M. Pignanelli, G. Pollarolo, A. DeRosa, G. Inglima, M. La Commara, G. La Rana, D. Pierroutsakou, M. Romoli, M. Sandoli, P. Bizzeti, A. Bizzeti-Sona, G. Lo Bianco, C. Petrache, A. Zucchiatti, P. Cocconi, B. Quintana, C. Beck, D. Curien, G. Duchene, F. Haas, P. Medina, P. Papka, J. Durell, S. Freeman, A. Smith, B. Varley, K. Fayz, V. Pucknell, J. Simpson, W. Gelletly, P. Regan, Coupling a clover detector array with the prisma magnetic spectrometer, The European Physical Journal A - Hadrons and Nuclei 20 (1) (2003) 193–197. doi:10.1140/epja/i2002-10352-9.

[14] K. Sieja, F. Nowacki, K. Langanke, G. Martinez-Pinedo, Shell model description of zirconium isotopes, Phys. Rev. C 79 (2009) 064310. doi:10.1103/PhysRevC.79.064310.

[15] S. Dimitrova, D. Bianco, N. Lo Iudice, F. Andreozzi, A. Porrino, Shell-model calculations for ^{91}Zr, Nuclear Theory 30 (2011) 100–105.

[16] S. Szilner, L. Corradi, F. Haas, D. Lebhertz, G. Pollarolo, C. A. Ur, L. Angus, S. Beghini, M. Bouhelal, R. Chapman, E. Caurier, S. Courtin, E. Farnea, E. Fioretto, A. Gadea, A. Goasduff, D. Jelavić-Malenica, V. Kumar, S. Lunardi, N. Mărginean, P. Mason, D. Mengoni, G. Montagnoli, F. Nowacki, F. Recchia, E. Sahin, M.-D. Salsac, F. Scarlassara, R. Silvestri, J. F. Smith, N. Soić, A. M. Stefanini, J. J. Valiente-Dobón, Interplay between single-particle and collective excitations in argon isotopes populated by transfer reactions, Phys. Rev. C 84 (2011) 014325. doi:10.1103/PhysRevC.84.014325.

[17] S. Lunardi, S. M. Lenzi, F. D. Vedova, E. Farnea, A. Gadea, N. Mărginean, D. Bazzacco, S. Beghini, P. G. Bizzeti, A. M. Bizzeti-Sona, D. Bucurescu, L. Corradi, A. N. Deacon, G. d. Angelis, E. Fioretto, S. J. Freeman, M. Ionescu-Bujor, A. Iordachescu, P. Mason, D. Mengoni, G. Montagnoli, D. R. Napoli, F. Nowacki, R. Orlandi, G. Pollarolo, F. Recchia, F. Scarlassara, J. F. Smith, A. M. Stefanini, S. Szilner, C. A. Ur, J. J. Valiente-Dobón, B. J. Varley, Spectroscopy of neutron-rich Fe isotopes populated in the ^{64}Ni+^{238}U reaction, Phys. Rev. C 76 (2007) 034303. doi:10.1103/PhysRevC.76.034303.

[18] F. Recchia, S. M. Lenzi, S. Lunardi, E. Farnea, A. Gadea, N. Mărginean, D. R. Napoli, F. Nowacki, A. Poves, J. J. Valiente-Dobón, M. Axiotis, S. Aydin, D. Bazzacco, G. Benzoni, P. G. Bizzeti, A. M. Bizzeti-Sona, A. Bracco, D. Bucurescu, E. Caurier, L. Corradi, G. de Angelis, F. Della Vedova, E. Fioretto, A. Gottardo, M. Ionescu-Bujor, A. Iordachescu, S. Leoni, R. Mărginean, P. Mason, R. Menegazzo, D. Mengoni, B. Million, G. Montagnoli, R. Orlandi, G. Pollarolo, E. Sahin, F. Scarlassara, R. P. Singh,

A. M. Stefanini, S. Szilner, C. A. Ur, O. Wieland, Spectroscopy of odd-mass cobalt isotopes toward the N=40 subshell closure and shell-model description of spherical and deformed states, Phys. Rev. C 85 (2012) 064305. doi:10.1103/PhysRevC.85.064305.

[19] S. Szilner, L. Corradi, F. Haas, G. Pollarolo, L. Angus, S. Beghini, M. Bouhelal, R. Chapman, E. Caurier, S. Courtin, E. Farnea, E. Fioretto, A. Gadea, A. Goasduff, D. Jelavić-Malenica, V. Kumar, S. Lunardi, N. Mărginean, D. Mengoni, T. Mijatović, G. Montagnoli, F. Recchia, E. Sahin, M.-D. Salsac, F. Scarlassara, J. F. Smith, N. Soić, A. M. Stefanini, C. A. Ur, J. J. Valiente-Dobón, Structure of chlorine isotopes populated by heavy ion transfer reactions, Phys. Rev. C 87 (2013) 054322. doi:10.1103/PhysRevC.87.054322.

[20] B. N. Laboratory, National nuclear data center, brookhaven national laboratory (2014).
URL http://www.nndc.bnl.gov/

[21] E. K. Warburton, J. W. Olness, C. J. Lister, R. W. Zurmühle, J. A. Becker, High-spin state spectroscopy of ^{88,90}Zr, Phys. Rev. C 31 (1985) 1184–1210. doi:10.1103/PhysRevC.31.1184.

[22] L. Corradi, S. Szilner, G. Pollarolo, G. Colò, P. Mason, E. Farnea, E. Fioretto, A. Gadea, F. Haas, D. Jelavić-Malenica, N. Mărginean, C. Michelagnoli, G. Montagnoli, D. Montanari, F. Scarlassara, N. Soić, A. M. Stefanini, C. A. Ur, J. J. Valiente-Dobón, Single and pair neutron transfers at sub-barrier energies, Phys. Rev. C 84 (2011) 034603. doi:10.1103/PhysRevC.84.034603.

[23] J. Sinatkas, L. D. Skouras, D. Strottman, J. D. Vergados, Shell-model calculations in the A=80-100 mass region: II. a study of the N=49, 48 nuclei, Journal of Physics G: Nuclear and Particle Physics 18 (8) (1992) 1401.

[24] D. K. Sharp, B. P. Kay, J. S. Thomas, S. J. Freeman, J. P. Schiffer, B. B. Back, S. Bedoor, T. Bloxham, J. A. Clark, C. M. Deibel, C. R. Hoffman, A. M. Howard, J. C. Lighthall, S. T. Marley, A. J. Mitchell, T. Otsuka, P. D. Parker, K. E. Rehm, D. V. Shetty, A. H. Wuosmaa, Neutron single-particle strength outside the N=50 core, Phys. Rev. C 87 (2013) 014312. doi:10.1103/PhysRevC.87.014312.

[25] C. R. Bingham, M. L. Halbert, Neutron shell structure in ^{91}Zr and ^{92}Zr by (d,p) and $(\alpha,\ ^3\mathrm{He})$ reactions, Phys. Rev. C 2 (1970) 2297–2309. doi:10.1103/PhysRevC.2.2297.

[26] H. Block, L. Hulstman, E. Kaptein, J. Blok, Investigation of ^{91}Zr by high resolution (d,p), (p,p') and (p,d) reactions, Nuclear Physics A 273 (1) (1976) 142 – 171. doi:http://dx.doi.org/10.1016/0375-9474(76)90305-5.

[27] C. R. Bingham, G. T. Fabian, Neutron shell structure in ^{93}Zr, ^{95}Zr, and ^{97}Zr by (d, p) and $(\alpha, {}^3\mathrm{H})$ reactions, Phys. Rev. C 7 (1973) 1509–1518. doi:10.1103/PhysRevC.7.1509.

[28] D. Beaumel, S. Fortier, S. Gals, J. Guillot, H. Langevin-Joliot, H. Laurent, J. Maison, J. Vernotte, J. Bordewijck, S. Brandenburg, A. Krasznahorkay, G. Crawley, C. Massolo, M. Renteria, A. Khendriche, Decay properties of high-lying single-particles modes, Nuclear Physics A 599 (12) (1996) 265 – 270. doi:http://dx.doi.org/10.1016/0375-9474(96)00068-1.

[29] S. T. Thornton, D. E. Gustafson, J. L. C. Ford, K. S. Toth, D. C. Hensley, Inelastic scattering and transfer reactions from ^{12}C ions on ^{90}Zr, Phys. Rev. C 13 (1976) 1502–1509. doi:10.1103/PhysRevC.13.1502.

[30] D. Pantelica, I. G. Stefan, N. Nica, M. G. Porquet, G. Duchêne, A. Astier, S. Courtin, I. Deloncle, F. Hoellinger, A. Bauchet, N. Buforn, L. Donadille, O. Dorvaux, J. Duprat, B. J. P. Gall, C. Gautherin, T. Kutsarova, S. Lalkovski, R. Lucas, M. Meyer, A. Minkova, A. Prévost, N. Redon, N. Schulz, H. Sergolle, O. Stézowski, T. Venkova, A. Wilson, High-spin states in $^{92-94}$Zr nuclei, Phys. Rev. C 72 (2005) 024304. doi:10.1103/PhysRevC.72.024304.